NOTAS DE FÍSICA

VOLUME XII

Nº 16

EXTENSIVE AIR SHOWERS OBSERVED IN THE EMULSION CHAMBER

by

M. Akashi, Z. Watanabe, J. Nishimura, K. Niu
T. Taira, N. Ogita, K. Ogata, Y. Tsuneoka, K. Shirai,
A. Misaki, I. Mito, K. Nishikawa, Y. Oyama, S. Hazama,
A. Nishio, I. Ota, S. Dake, K. Yokoi, M. Sakata, T. Yuda,
K. Mizutani, Y. Fujimoto, S. Hasegawa, A. Osawa, T. Shibata,
T. Suzuki, C. M. G. Lattes, C. Q. Orsini, I. G. Pacca,
M. T. Cruz, E. Okuno, T. Borello, M. Kawabata,
and A. M. Endler

CENTRO BRASILEIRO DE PESQUISAS FÍSICAS

Av. Wenceslau Braz, 71

RIO DE JANEIRO

1967

Notas de Física - Volume XII - Nº 16

EXTENSIVE AIR SHOWERS OBSERVED IN THE EMULSION CHAMBER III

M. Akashi, Z. Watanabe
Hirosaki University

J. Nishimura, K. Niu, T. Taira
Institute for Nuclear Study

N. Ogita
Institute of Phys. and Chem. Research

K. Ogata, Y. Tsuneoka, K. Shirai
Kwansei Gakuin University

A. Misaki, I. Mito, K. Nishikawa, Y. Oyama, S. Hazama
Konen University

A. Nishio
Kyoto University

I. Ota, S. Dake, K. Yokoi, M. Sakata, T. Yuda, K. Mizutani
Nagoya University

Y. Fujimoto, S. Hasegawa, A. Osawa, T. Shibata, T. Suzuki
Waseda University

C. M. G. Lattes, C. Q. Orsini, I. G. Pacca, M. T. Cruz,
E. Okuno, T. Borello, M. Kawabata,
S. Hasegawa*, J. Nishimura*
Universidade de São Paulo

A. M. Endler
Centro Brasileiro de Pesquisas Físicas

(Received January 19, 1967)

---

* Staying in São Paulo at the first stage of the analysis.

ABSTRACT

Large emulsion chambers (about 10 m^2 area) exposed at mountain altitudes (5500 m and 2800 m) provides us means of observing the highest energy particles of EAS cores. Lateral distribution of the high energy γ rays in a cascade shower, properties of successive interactions in the atmosphere, and analysis of the core structure are discussed using the data observed in our chamber.

* * *

Families of gamma-rays and jets observed in our large emulsion chambers are the cores of EAS in earlier stages of their development, and give us valuable information on the structure of EAS. The area of our chamber (~ 6 m^2) is large enough to catch extremely high energy events, and a few events of total energies $\gtrsim 10^{15}$ eV can be expected to be observed during the exposure of about one year. High spatial resolving power of our chamber ($\sim 50\,\mu$) make us possible to measure accurately locations. This, together with good accuracy of energy determination one can make detailed analysis and get precise information on EAS cores by the chamber which would not be obtainable by the ordinary EAS aparatus. The design of chambers and the list of exposures are given in separate papers. [1, 2, 3]

Classification of Events

Figure 1 shows several typical examples of families observed in our chamber. In Fig. 1A, one sees a large cascade shower of complex nature which is probably originated from a π^0-meson of $\sim$100 TeV produced at a high altitude. In fig. 1B, is given an example of a family with large number of Pb jets. Figure 1C shows an event interpreted as an atmospheric interaction occured near the chamber so that these is no significant effect of cascade multiplication during the traverse through the atmosphere. Even if γ rays decayed from π^0 mesons are suffered by the cascade processes, one can identify the individual resultant cascade showers in the events occurring not beyond 3 cascade units from our chamber. Hereafter we shall call these individual cascade showers as air cascades.

Lateral Distributions of Particles in Air Cascades

Figure 2 gives a plot of energy E and distance R of γ-rays and electrons from the center of an air cascade. The statistics are based on 37 air cascades containing three or more constituent particles. The lateral distribution can be given in a form independent of the incident energy, when one measures the distance in the unit equal to (K/E) times a cascade unit in air. Figure 3 shows the lateral distribution of the shower particles expressed by the above unit. Theoretical curves obtained from the three dimensional cascade theory of Nishimura and Kamata [4] for ages 1.0, 1.4 and 2.0 are also shown in the figure. The

comparison of the experimental distribution with the theoretical ones indicates that the shower age of the observed air cascades lying between 1.0 and 1.4.

The expected shower age from the analysis of the attenuation length (110 ± 10) g cm^{-2} is about 1.4. The slight discrepancy between the observed and the expected values may be due to the facts that we omitted the small size shower and that we took the center of energy of shower particles as the axis.

Successive Interaction in Air

Many successive events were observed in our chamber among high energy atmospheric interactions of total γ-ray energy $\sum E_\gamma \geqslant 2.10^{13}$ eV. From the analysis of the spread of air cascades and by the coupling of the two γ-rays into π^o-meson, [1] one can estimate the originating points of nuclear interactions and separate groups of particles which belong to different generations.

Figure 4 shows the energy-hight relations for observed successive events for $\sum E_\gamma \geqslant 10^{13}$ eV. The chain lines in the figure indicate the average lines of successive interactions expected under an assumption of constant inelasticities K = 0.3, 0.5 and 0.7. The constant values assumed for K correspond to those obtained from the geometric means of the elasticities (1 - K) in all successive events.

The solid curves in Fig. 4 indicate lines at which produced γ rays with energy 0.1 times of ΣE_γ are detected with a probability of 0.1, 0.2 and 0.5. [1] Only few events including three or more

generations were observed, and this makes us to expect that the average inelasticity is smaller than 0.7. Furthermore, detailed analysis about the ratio of energy liberated in the form of γ-rays to that liberated by a survival nucleons giving us the information of the value of K. The average value of K thus obtained is about 0.5 as shown in the reference 3.

Core Structure of EAS

Many EAS with double or multiple core structure of the mutual distance $\sim$1 m have been observed by several groups.[5~9] Some of them have interpreted that multiple core structure is caused from the large transverse momenta of produced particles and others[8] proposed that the core structure is due to a heavy primary particle.

Atmospheric depths from Mt. Chacaltaya (5200 m) and Mt. Norikura (2800 m) to sea level are 12 and 8 cascade units respectively. Then, γ-ray families observed in our chambers are the early stage of the cores of EAS observed at sea level and offer information on its detailed structure. Two examples of families with large $P_{T\pi^0}$ are selected out of about 30 events of higher energy. Their cascade development is traced down to the sea level with use of the theoretical lateral distribution without Landau's approximation calculated by Nishimura.[4] Fig. 5 shows sketch of the two events together with their expected lateral distribution of electrons near the core at sea level. The two examples show the multiple core structure.

Therefore, one should expect that several percent of EAS will show the multiple core structure originating from large P_T in the nuclear interaction.

Primary Spectrum

The observation of nuclear interactions in the chamber provides flux values of nucleon component at the mountain altitude.[1] The primary proton flux are estimated from the data assuming the absorption mean free path as 110 ± 10 g/cm^2. The conversion factor of the liberated energy of nuclear interactions, ΣE_γ, into the incident nucleon energy is taken as $1/K_\gamma = 4 \sim 6$.[2, 3] Errors in the absolute determination of energy will be at most 20%. Figure 6 shows the primary flux value obtained with combined probable errors.

The analysis on large families observed in our chamber gives also the nucleon flux value at higher altitudes. We present in Fig. 6 the value estimated from the three events of the highest energy occurred within 2 Km from the chamber. * This highest energy point is consistent with an extrapolation of the above results.

Discussions

As discussed in this report, the energy range of interactions observed by the emulsion chamber is now close to the EAS region, and analysis has shown that information from the direct observation can provide new perpspective in understanding the EAS phenomena.

* See Appendix.

Let us now discuss on the primary cosmic-ray particles.

The primary flux value estimated from the present experiment are found consistent with the results of other laboratories using a similar apparatus. As is seen in Fig. 6, there is indication that these values are systematically lower than extrapolation of the value obtained from the EAS experiment. Though a comparison of absolute values of experiments of different character have to be taken carefully, one may look for a possible cause of the systematic deviation. The EAS experiment measures flux of energy of incoming particles irrespectively whether it is a proton or a heavy nuclei. As estimation on effects of heavy primaries shows that the proton flux should be about a half of the quoted value at high energy if the composition does not change with energy. On the other hand, experiment on the nucleon flux, such as the present experiment, will be affected only slightly by existence of heavy primary particles. This may explain the observed disdrepancy.

* * *

APPENDIX I - Examples of Atmospheric Interactions of the Highest Energy

One is able to observe several generations of interactions as its energy becomes higher. Analysis of those high energy events gives us general picture on the nucleon cascades.

Selecting three events of the highest energy originated within distance $\leqslant 2$ Km from the detector, results of the analysis are presented in Fig. 7. We observe 3 generations for one event and 4 generations for the other two. These examples will help us in understanding the mechanism governing development of EAS.

* * *

Captions of Figures

Fig. 1: Typical examples of families in our chambers.
A: large cascade shower of complex nature;
B: family with large number of jets in Pb plates;
C: clear jet event.

Fig. 2: Energy-radial distance distributions of γ rays and electrons in air cascades.

Fig. 3: Experimental and theoretical lateral distributions of air cascade.

Fig. 4: Energy-height distribution of observed successive atmospheric interactions.

Fig. 5: Sketch of the typical families causing the multiple core events and their expected lateral distributions of electrons near the cores at sea level.

Fig. 6: Primary spectrum
— : extrapolation of the EAS data;
o : present experiment on Pb jets;
▨ : estimated value from the Pb jet data;
× : estimated value from the large γ-ray families;
● : results of Bristol group ; [10]

△ : results of Moscow group.[11]

Fig. 7: Illustration of the results of the analysis on Atmospheric interactions of the highest energy.

* * *

REFERENCES:

1. M. AKASHI et al., Suppl. Prog. Theor. Phys., in press.
2. M. AKASHI et al., in this Proceedings.
3. M. AKASHI et al., in this Proceedings.
4. J. NISHIMURA, Handbuch der Physik, in press.
5. R. E. HEINEMANN and W. E. HAZEN, Phys. Rev. 90, 496 (1953).
   R. E. HEINEMANN, Phys. Rev. 96, 161 (1959).
6. N. N. GORGUNOV et al., Proc. of Moscow Conf., 2, 70 (1960).
7. M. ODA and Y. TANAKA, J. Phys. Soc. Japan, 17, Suppl. A-III, 282.
   S. MIYAKE et al., J. Phys. Soc. Japan, 17, Suppl. A-III, 266.
8. C. B. A. MC CUSKER et al., Nuovo Cimento, 31, 525 (1964).
9. S. MIYAKE et al., in this Proceedings.
10. L. T. BRADZEI et al., J. Phys. Soc. of Japan, 17, Suppl. A-III, 433.
11. M. BOWLER et al., J. Phys. Soc. of Japan, 17, Suppl. A-III, 424.

* * *

Family 19-I

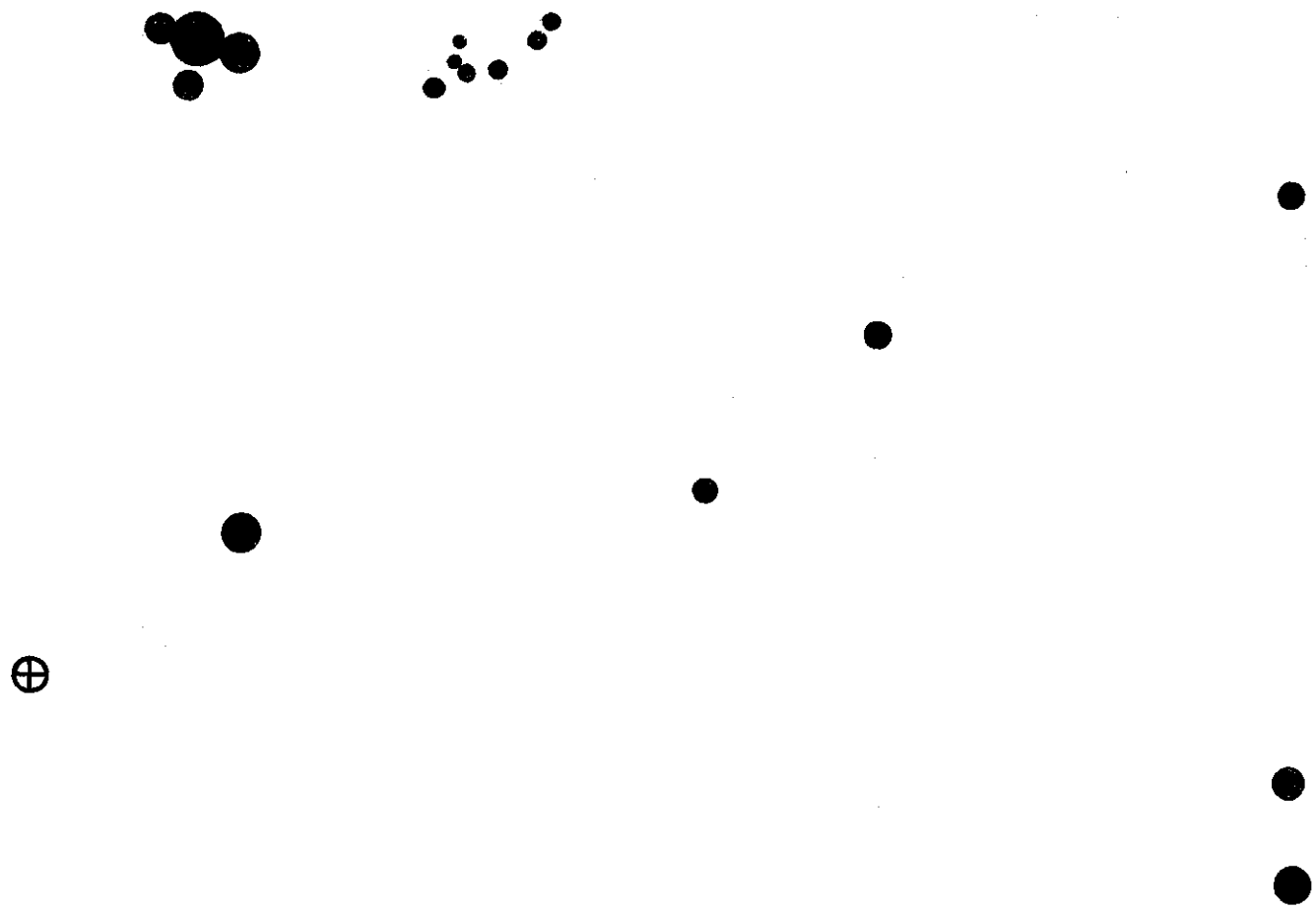

Fig. 1

21 - F3

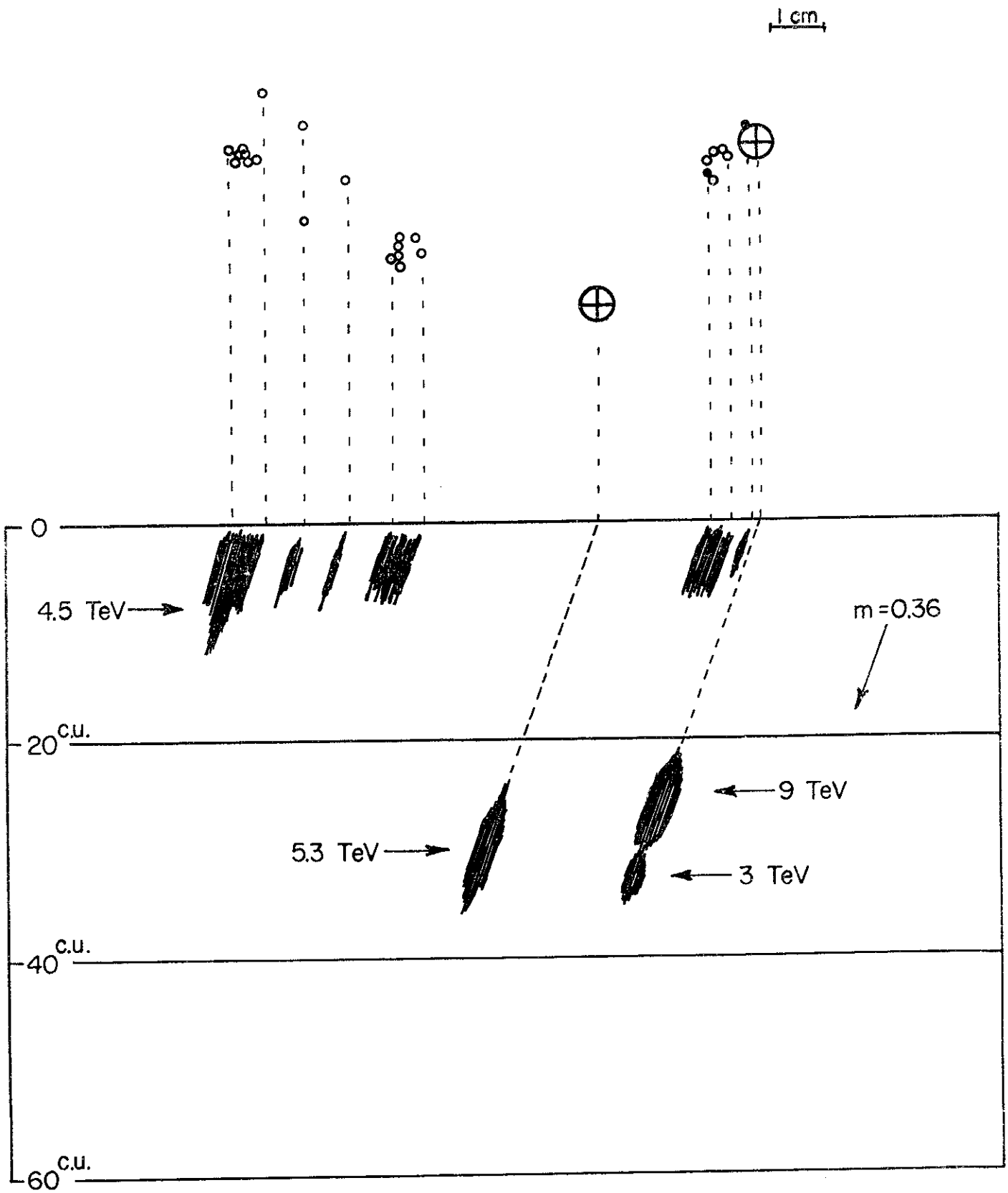

Fig. 1A

Family 21-I

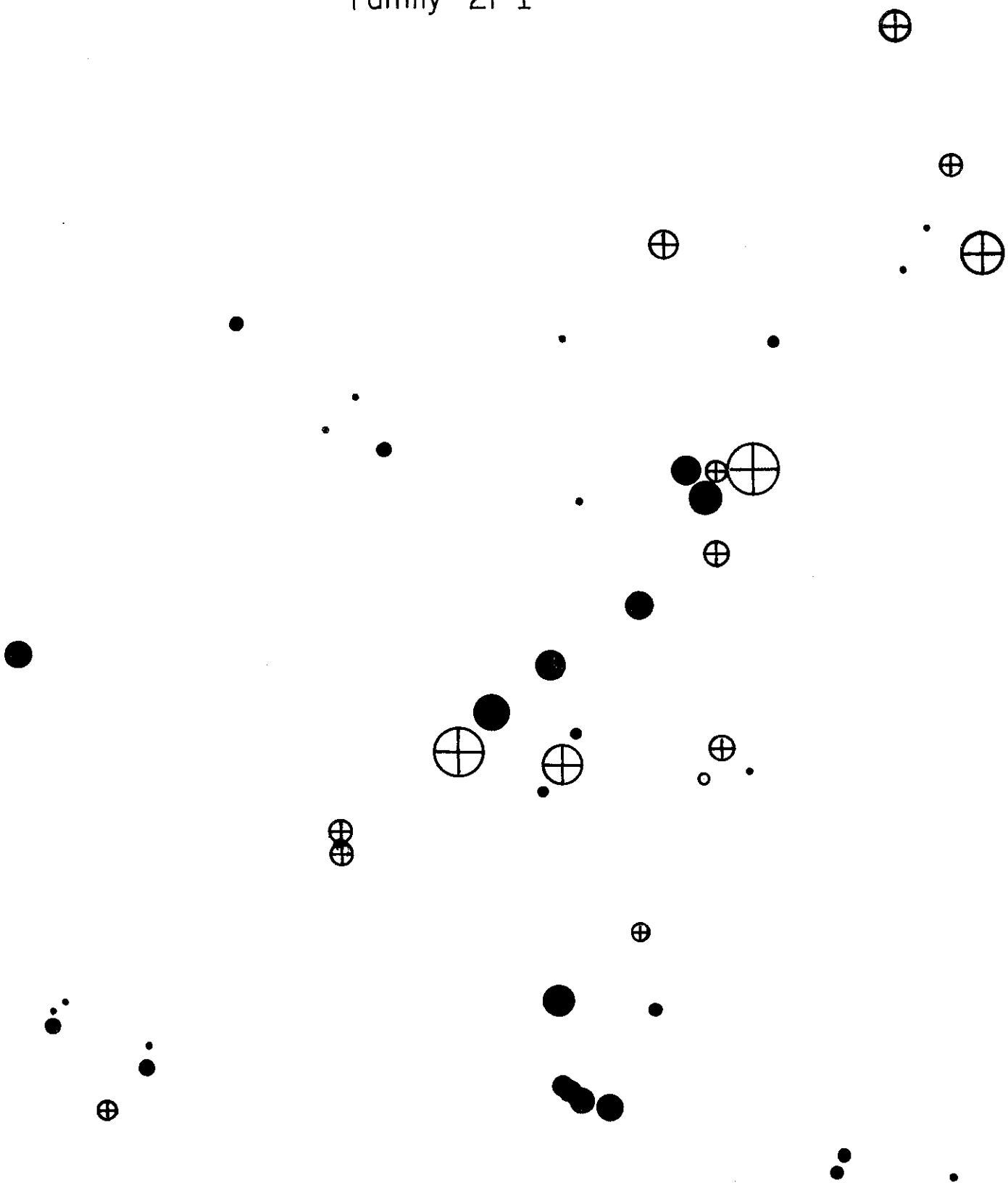

Fig. 1B

21 - IIA

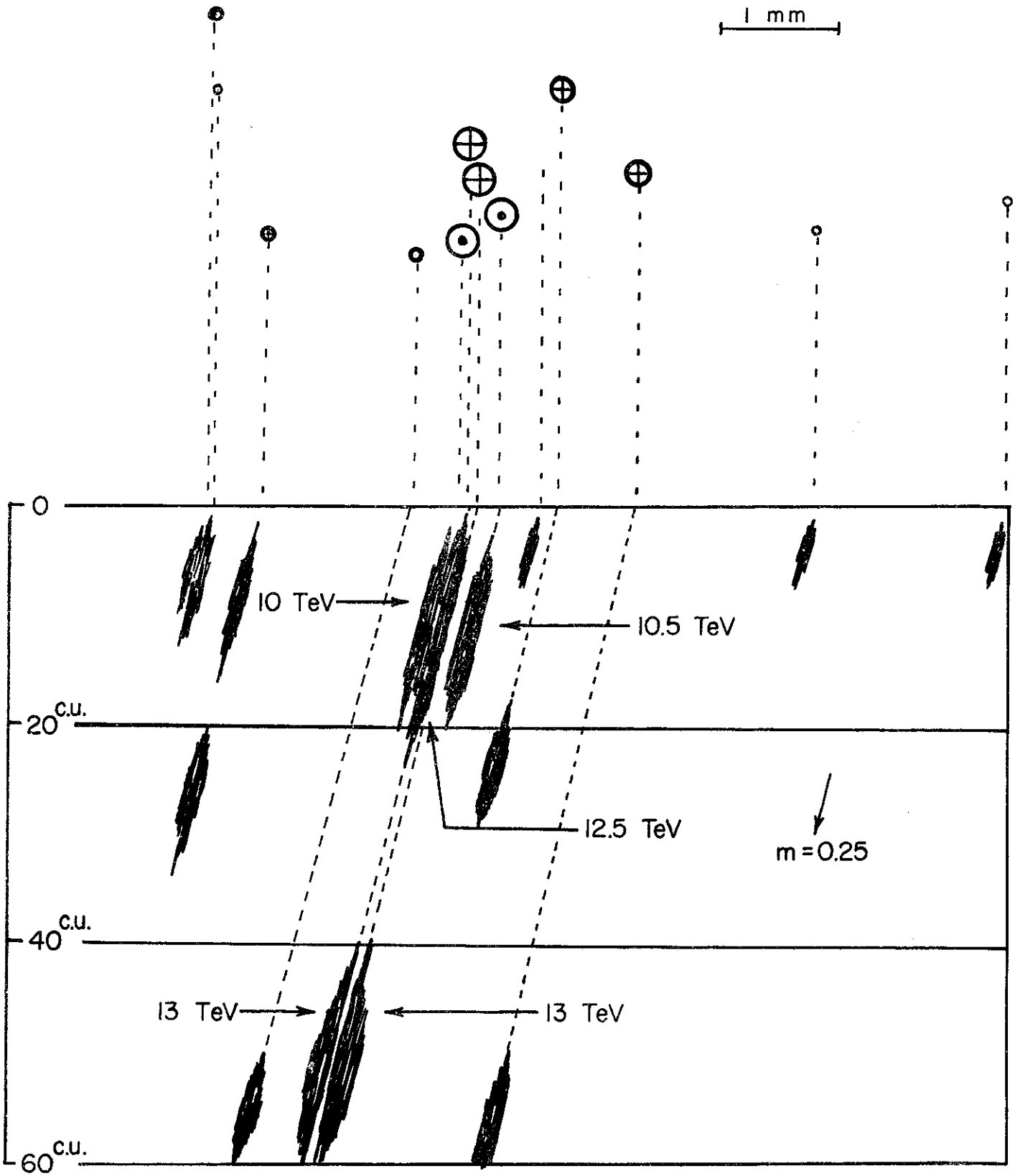

Fig. 1C

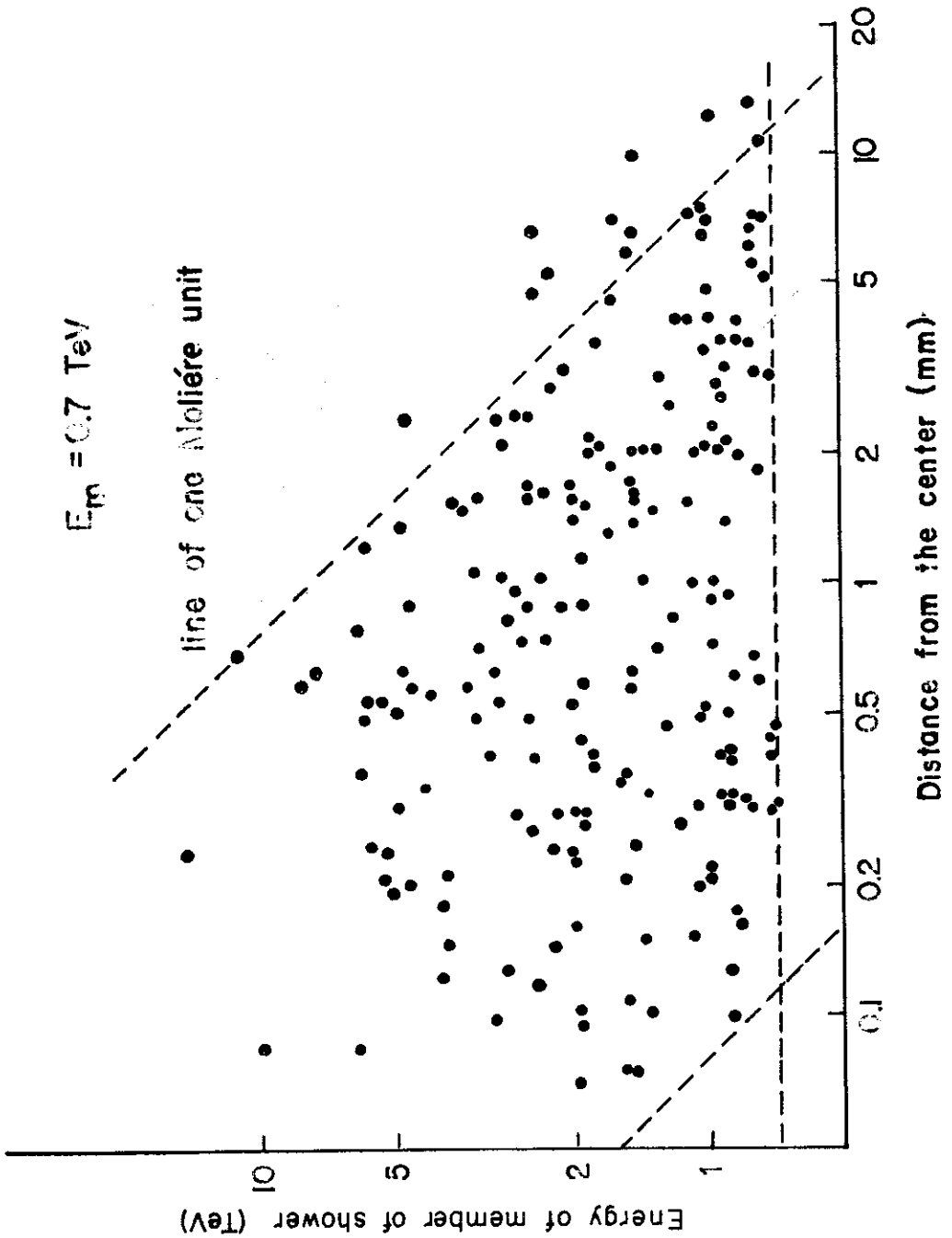
E_m = 0.7 TeV
line of one Moliére unit
Energy of member of shower (TeV)
10
5
2
1
0.1
0.2
0.5
1
2
5
10
20
Distance from the center (mm)

Fig. 2

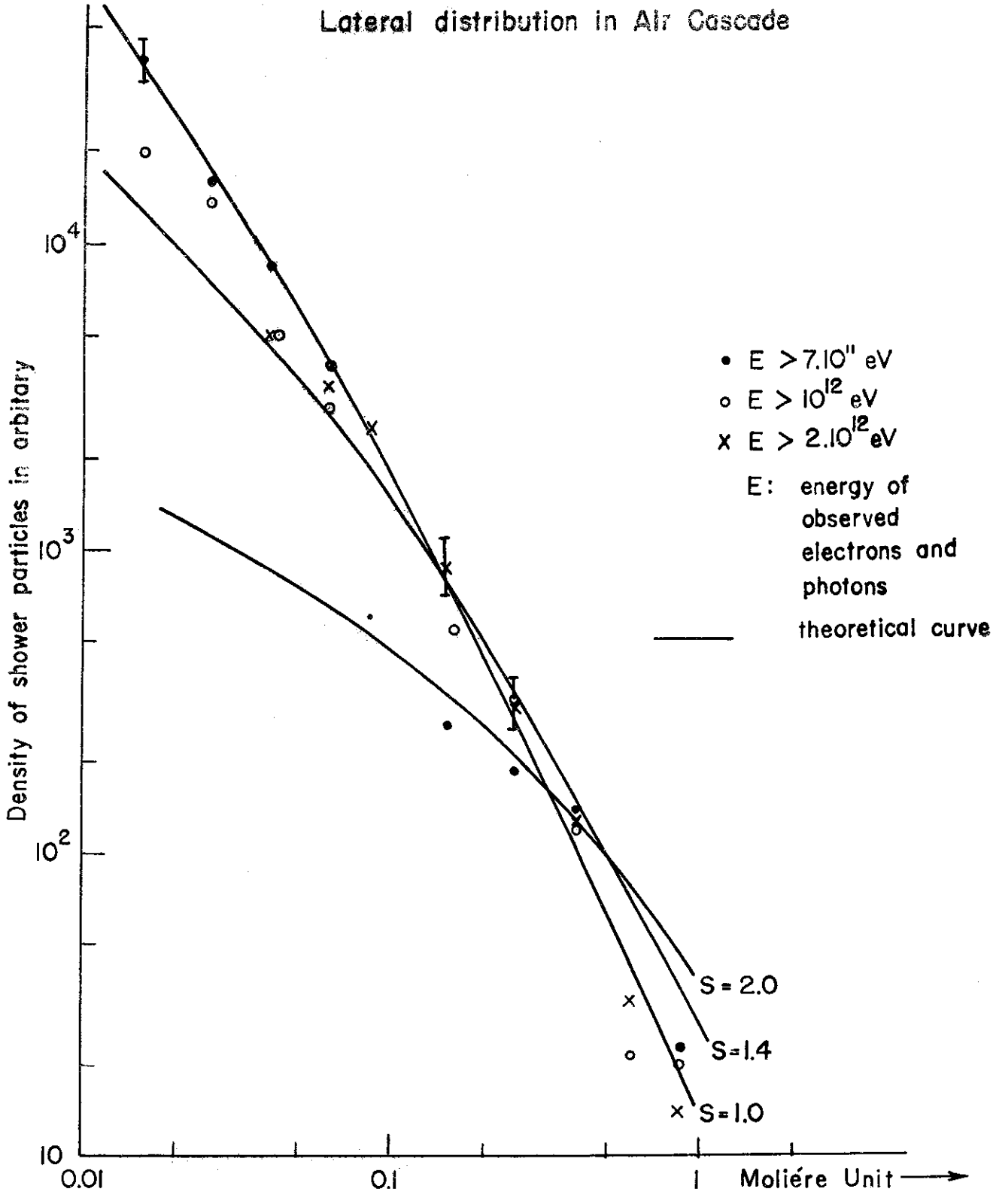
Lateral distribution in Air Cascade
Density of shower particles in arbitary
10^4
10^3
10^2
10
0.01
0.1
1
Moliére Unit
• E > 7.10^11 eV
o E > 10^12 eV
x E > 2.10^12 eV
E: energy of observed electrons and photons
theoretical curve
S = 2.0
S=1.4
S=1.0

Fig. 3

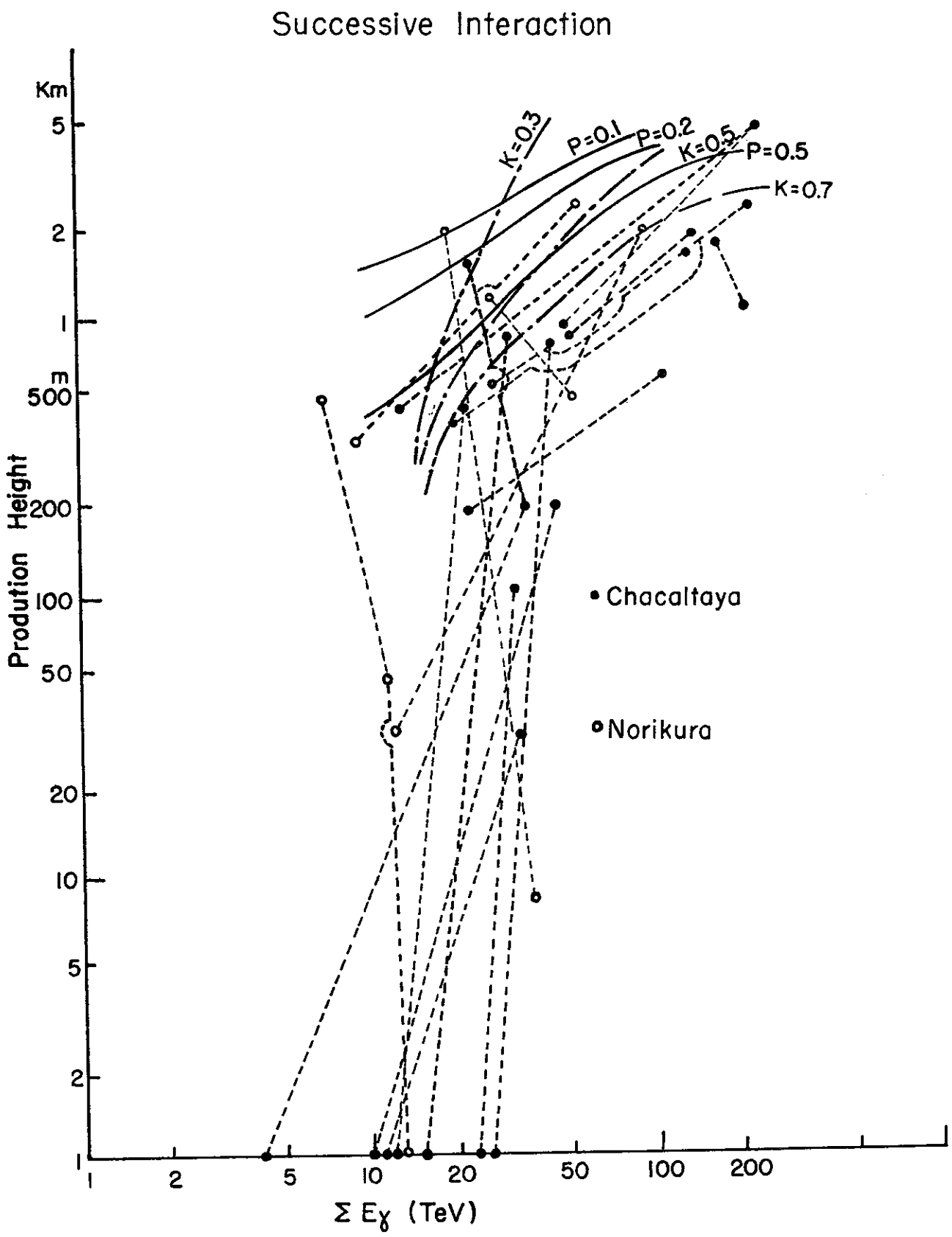
Successive Interaction
Km
5
2
1
m
500
200
100
50
20
10
5
2
1
Prodution Height
K=0.3
P=0.1
P=0.2
K=0.5
P=0.5
K=0.7
• Chacaltaya
o Norikura
1
2
5
10
20
50
100
200
Σ Eγ (TeV)

Fig. 4

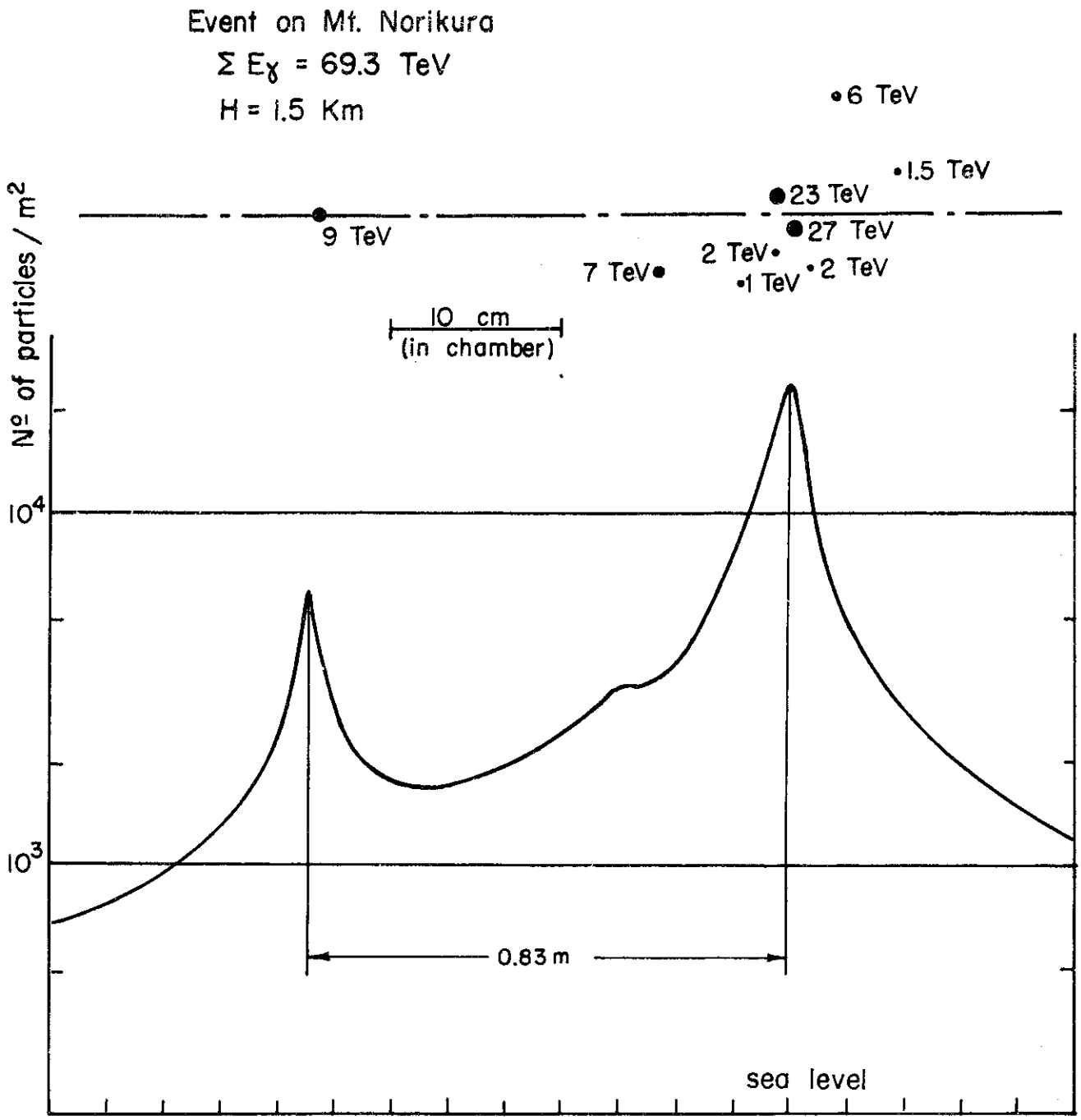
Event on Mt. Norikura
Σ Eγ = 69.3 TeV
H = 1.5 Km
6 TeV
1.5 TeV
23 TeV
27 TeV
2 TeV
2 TeV
1 TeV
7 TeV
9 TeV
10 cm
(in chamber)
Nº of particles / m²
10⁴
10³
0.83 m
sea level

Fig. 5A

Event on Mt. Chacaltaya
ΣE_γ = 40.5 TeV
H = 210 m

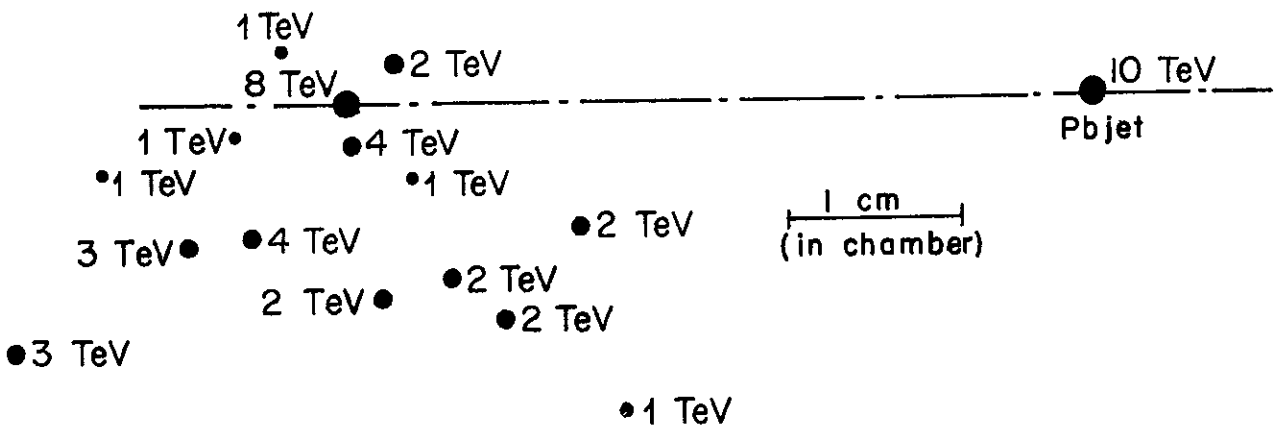

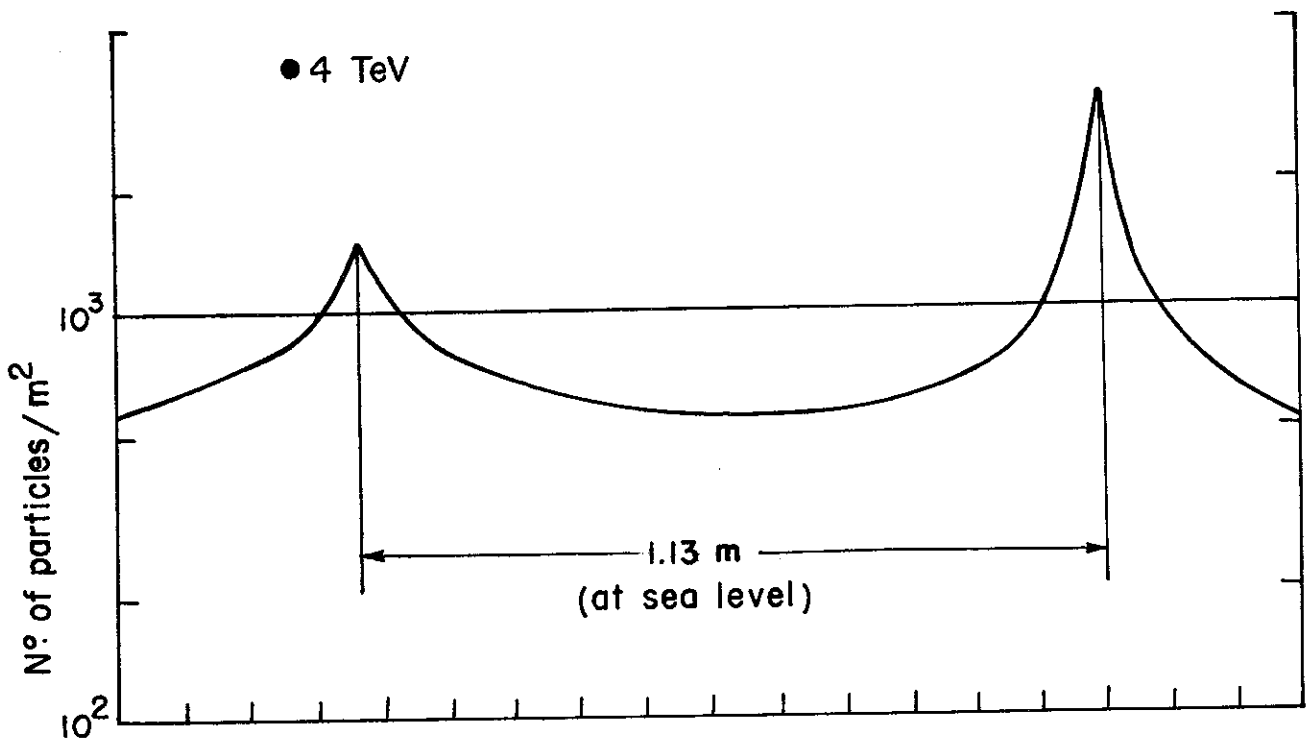

Fig. 5B

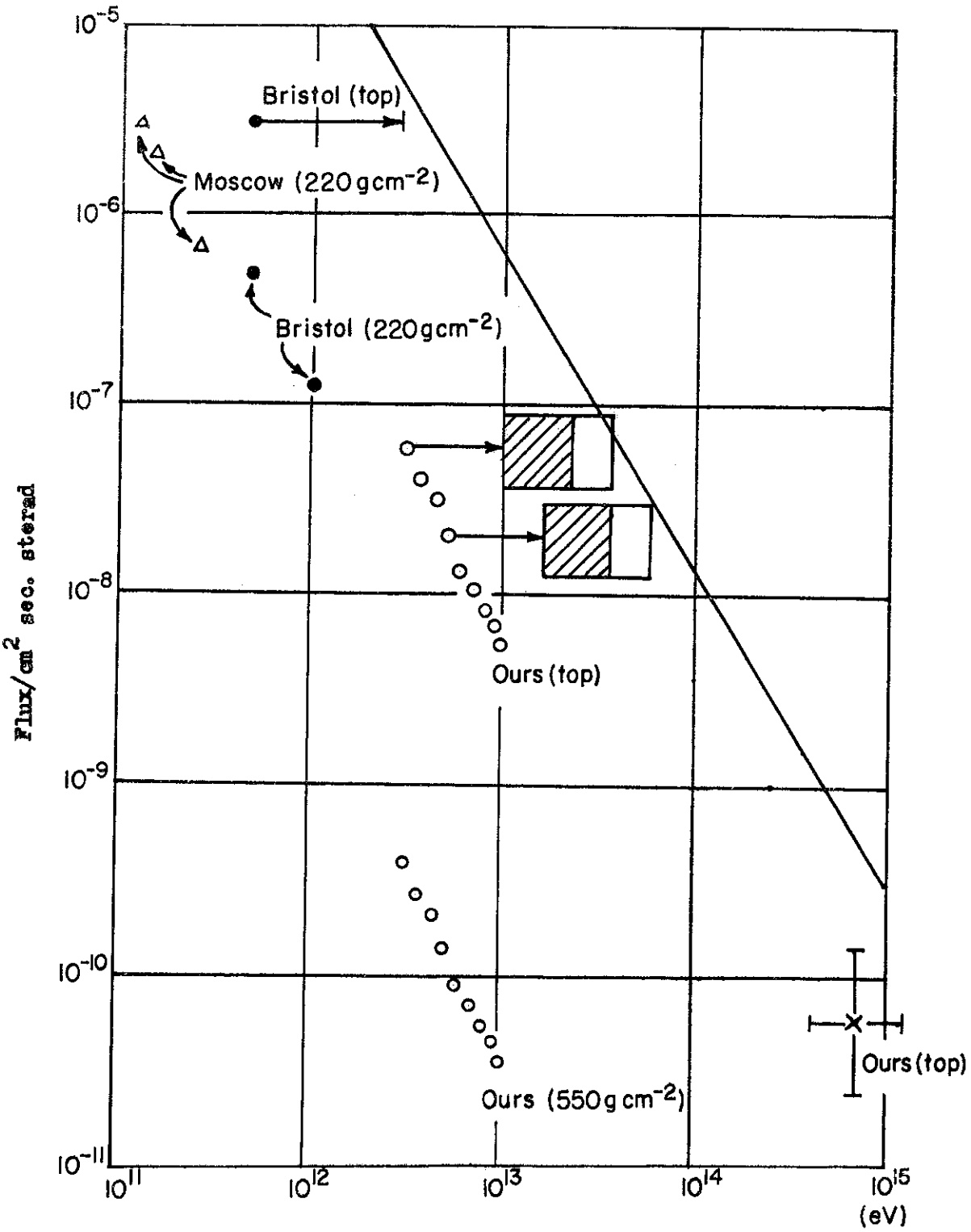
Bristol (top)
Moscow (220 g cm⁻²)
Bristol (220 g cm⁻²)
Ours (top)
Ours (550 g cm⁻²)
Ours (top)
Flux/cm² sec. sterad
(eV)
10⁻⁵
10⁻⁶
10⁻⁷
10⁻⁸
10⁻⁹
10⁻¹⁰
10⁻¹¹
10¹¹
10¹²
10¹³
10¹⁴
10¹⁵

Fig. 6

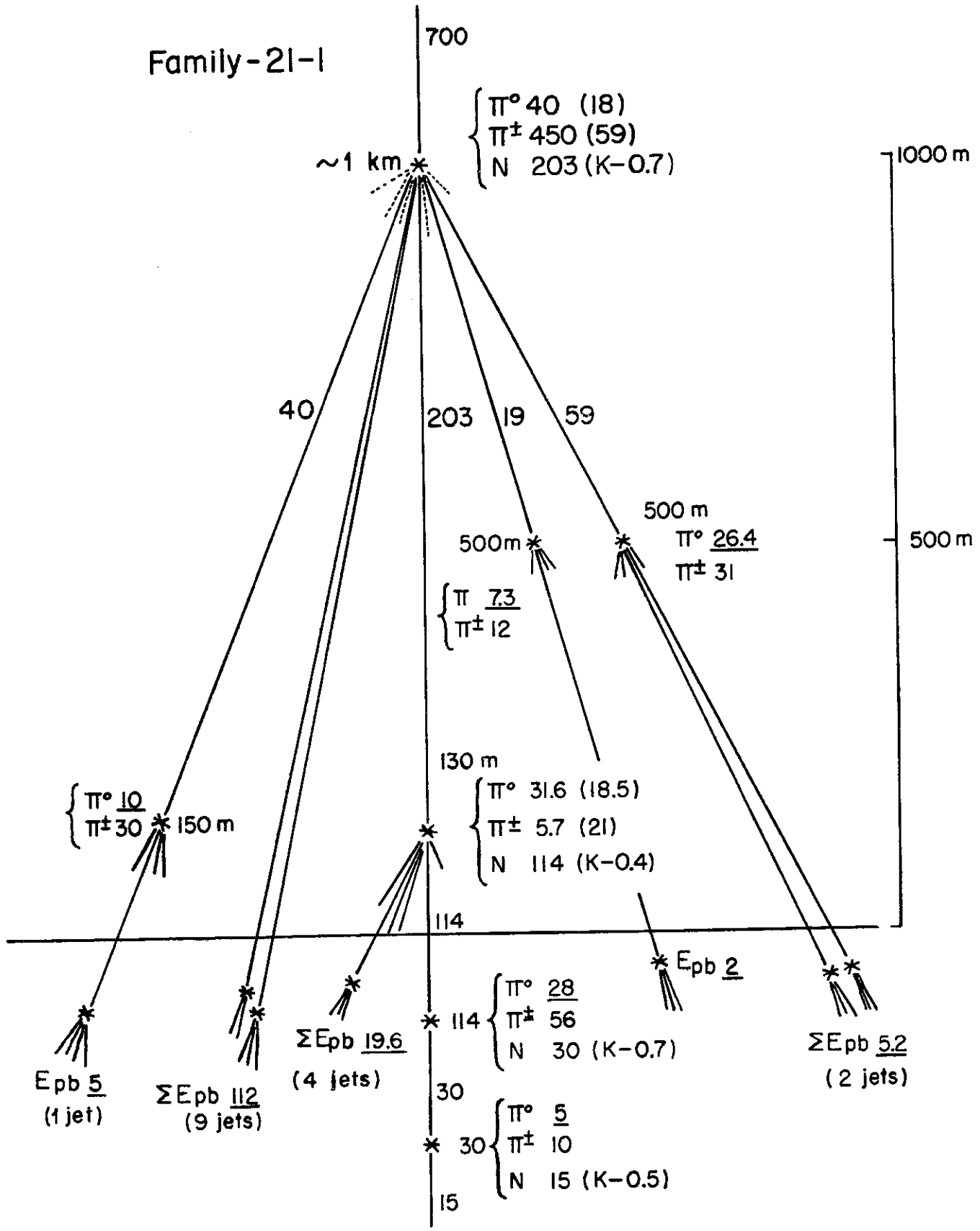
Family-21-1
700
~1 km
πº 40 (18)
π± 450 (59)
N 203 (K-0.7)
1000 m
500 m
40
203
19
59
500 m
πº 26.4
π± 31
500m
π 7.3
π± 12
130 m
πº 31.6 (18.5)
π± 5.7 (21)
N 114 (K-0.4)
πº 10
π± 30
150 m
114
Epb 2
ΣEpb 5.2
(2 jets)
114
πº 28
π± 56
N 30 (K-0.7)
ΣEpb 19.6
(4 jets)
Epb 5
(1 jet)
ΣEpb 112
(9 jets)
30
30
πº 5
π± 10
N 15 (K-0.5)
15

Fig. 7A

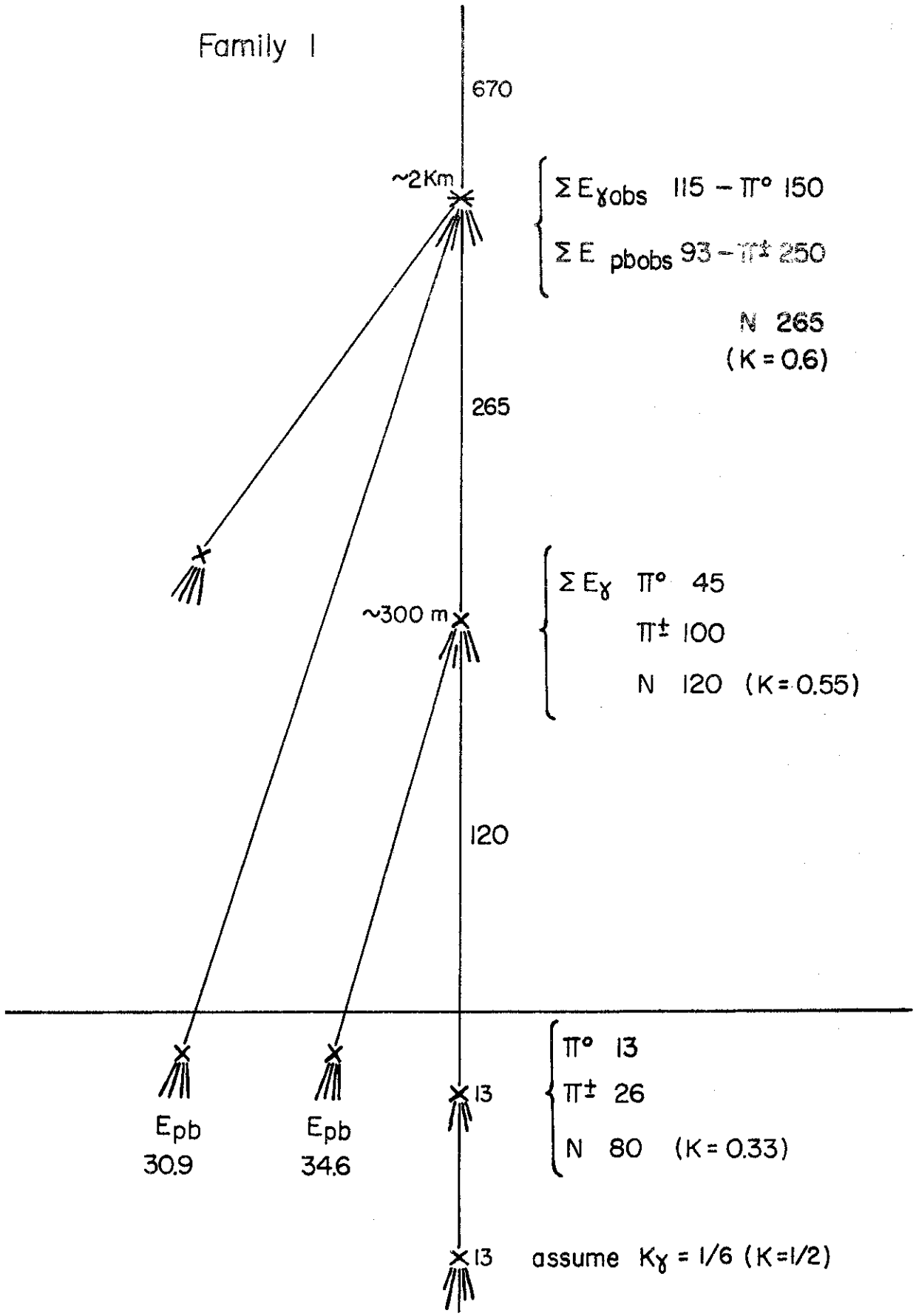
Family I
670
~2Km
Σ Eγobs 115 – π° 150
Σ E pbobs 93 – π± 250
N 265
(K = 0.6)
265
~300 m
Σ Eγ π° 45
π± 100
N 120 (K = 0.55)
120
13
π° 13
π± 26
N 80 (K = 0.33)
Epb
30.9
Epb
34.6
13
assume Kγ = 1/6 (K = 1/2)

Fig. 7B

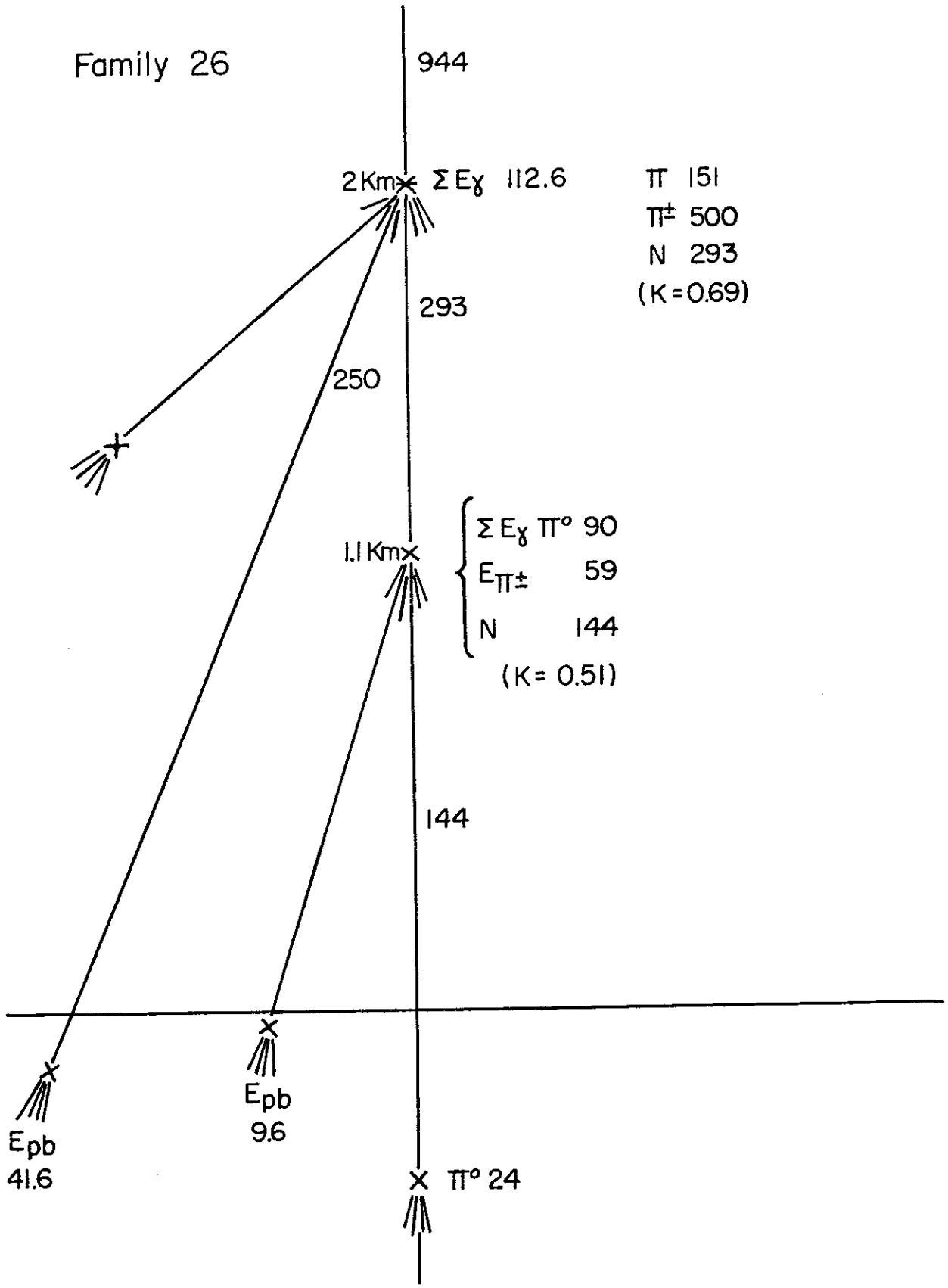
Family 26
944
2Km
Σ Eγ 112.6
π 151
π± 500
N 293
(K=0.69)
293
250
1.1Km
Σ Eγ π° 90
Eπ± 59
N 144
(K= 0.51)
144
Epb
41.6
Epb
9.6
π° 24

Fig. 7C